DOI: 10.53469/jpce.2024.06(07).04

Strain Prediction for High-Speed Rail Canopies in Cold Regions Based on LSTM Models

Changxin Guo[1,*], Xin Gao[1], Chunguang Lan[2]

[1]College of Construction Engineering, Jilin University, Changchun 130021, Jilin, China
[2]Beijing Construction Engineering Research Institute Co., LTD, Beijing 100039, China
Correspondence Author, cxguo22@mails.jlu.edu.cn

Abstract: ***With the rapid development of high-speed rail (HSR) in China, the platform canopies of HSR stations have become crucial structures for ensuring operational safety and providing sheltered waiting areas for passengers. Temperature variations, being the primary factor affecting structural strain, lead to internal temperature responses that significantly impact the health of these structures. Modern Structural Health Monitoring (SHM) systems collect structural response data to evaluate health status and detect anomalies in real time. With the advancement of data-driven models, machine learning, particularly deep learning, is increasingly applied in civil engineering. This study employs Recurrent Neural Networks (RNN) and Long Short-Term Memory (LSTM) networks to handle time series data, establishing a health monitoring and early warning system for HSR station canopies. The results demonstrate that deep learning models effectively capture the complex relationship between temperature and strain, enhancing the accuracy of strain variation predictions. This provides strong support for the safe operation of HSR station canopies.***

Keywords: Structural Health Monitoring, LSTM, Strain prediction**.**

1. Introduction

With the continuous development of Chinese high-speed rail (HSR), it has increasingly become an essential means of transportation for people. The platform awning of HSR stations serves as a crucial structure that ensures operational safety and provides sheltered waiting areas for passengers. Understanding the internal force variations within the awning structure is of paramount importance to managers. Therefore, it is imperative to establish an effective structural health monitoring and early warning system for HSR station canopies to ensure the safe operation of HSR [1]. Temperature is the primary factor causing strain variations in awning structures. Changes in external temperature affect the structure's internal temperature, leading to temperature responses within the structure. Over prolonged service periods, these temperature responses can have significant impacts [2-4].

Structural Health Monitoring (SHM) systems are capable of collecting data on structural responses, which are essential for evaluating the health status of structures and for the real-time detection of abnormal events. Consequently, there is a growing trend in installing advanced health monitoring systems in large-scale or critical civil infrastructure [5-6]. Additionally, numerous innovative detection techniques are being implemented in awning structures. Monitoring systems have accumulated vast amounts of environmental information and response data, shifting engineering research towards a data-driven model. Based on this extensive data, machine learning has gradually been applied in the field of civil engineering [7-10].

Deep learning technology, a pivotal subfield of machine learning, employs sophisticated neural network algorithms, particularly those associated with deep learning networks characterized by intricate architectures and refined cellular structures. These advancements endow deep learning networks with heightened generalization capacities for resolving complex input-output modeling challenges prevalent in highly nonlinear projects. To ameliorate the nonlinear fitting performance of neural networks concerning time series data, the deep learning Recurrent Neural Network (RNN) has emerged, specifically tailored to accommodate the temporal dependencies inherent in such data sequences. However, despite these advancements, the efficacy of RNNs remains constrained in scenarios demanding extensive data assimilation [11]. In response to challenges such as gradient vanishing and explosion encountered during neural network training, Long Short-Term Memory (LSTM) networks have been developed as an evolution of RNNs [12].

Notably, LSTM networks have been shown through empirical studies and engineering applications to exhibit robust inferential capabilities, particularly in modeling endeavors characterized by pronounced nonlinear input-output relationships. For instance, a real-time structural damage assessment methodology leveraging LSTM networks has been devised and validated for reliability on a physical bridge structure [7]. Furthermore, LSTM networks have demonstrated exceptional predictive accuracy in forecasting wind-induced vibration responses in lightning rod structures [10]. Additionally, an LSTM-based digital regression model, leveraging temperature data as input and deflection data as the response variable, has been proficiently tailored to capture intricate temperature-deflection relationships, surpassing the performance of conventional linear regression and multiple linear regression models [13]. Furthermore, the incorporation of an attention mechanism into a Bi-LSTM model has enabled the effective capture of spatial correlation features and temporal non-stationary response processes, thereby enhancing the predictive capabilities of the model [14]. Therefore, deep learning undoubtedly stands as a potent tool for addressing intricate engineering challenges.

2. Characteristics Analysis of Temperature and Strain Data

2.1 The Introduction of Platform Awning and Monitoring System of High-speed Railway

(a) Fuyu North Station

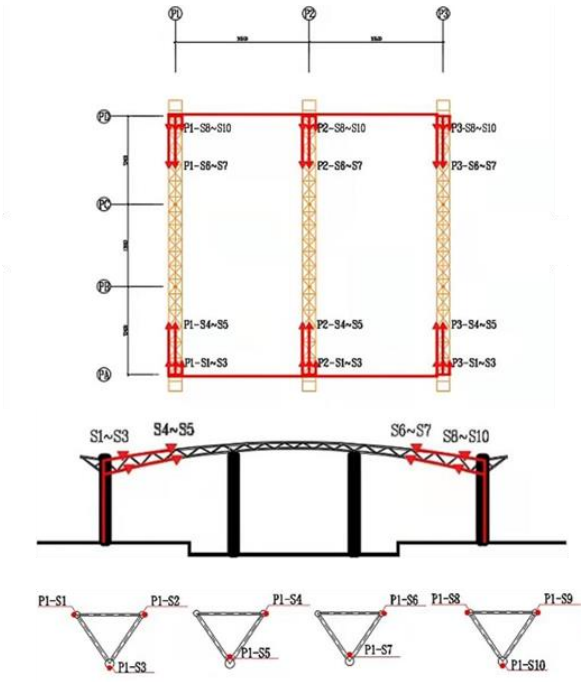

(b) Sensor layout diagram

Figure 1: Fuyu North Station and Monitoring System

This study focuses on the canopy structure of a high-speed rail station situated in a cold region, as illustrated in Figure 1(a). The structure is located in an area characterized by substantial seasonal temperature fluctuations and significant diurnal temperature variations. To comprehensively understand the static and dynamic properties as well as the long-term performance of the structure, and to facilitate effective long-term operation and maintenance management, a monitoring system has been implemented at Fuyu North Station.

This monitoring system collects data from the three trusses of Platform 1. As shown in Figure 1(b), a total of 30 strain and temperature sensors are installed at the specified measurement points on the trusses, labeled from P1-S1 to P3-S10. Sensors S1, S2, S4, S6, S8, and S9 are positioned on the upper chords of the structure, where they are more significantly affected by sunlight. In contrast, sensors S3, S5, S7, and S10 are located on the lower chords, where the influence of sunlight is less pronounced. Additionally, sensors S1 to S5 are situated on the shaded side of the structure, while sensors S6 to S10 are on the sunlit side.

For structural strain monitoring, the MOS-6301 vibrating wire surface strain gauge was chosen. This strain gauge is composed of flanges at both ends, a stainless steel pipe, and a steel wire passing through the pipe, all constructed from stainless steel. With a standard range of 3000με and a sensitivity of 1με, it operates within a temperature range of -20℃ to 80℃, perfectly meeting the requirements of monitoring systems. To ensure the reliability of long-term monitoring, it's essential to weld the sensor onto the structure being measured. To prevent sensor damage, the installation end block of the sensor should be welded to the structure under test prior to sensor installation. Once the sensor is installed, initial readings can be taken.

To monitor environmental variables, an integrated weather monitoring station is deployed outside the canopy. This station system integrates the collection, storage, transmission, and management of meteorological data, serving as an unattended meteorological collection system. Comprising meteorological sensors, meteorological data collectors, and computer meteorological software, the system can concurrently monitor atmospheric temperature, humidity, rainfall, wind speed, wind direction, air pressure, snow depth, and other meteorological parameters. In this study, the primarily utilized data are the monitored atmospheric temperature readings.

Figure 2: MOS-6301 Vibrating wire surface strain gauge

2.2 Analysis of the Correlation between Strain and Temperature

The atmospheric temperature measured by the monitoring system, also known as ambient temperature, undergoes periodic changes due to the movement of the sun. Consequently, there will be a maximum and a minimum value recorded each day, with the daily change trend generally consistent. Simultaneously, temperature sensors affixed to the structure capture the temperature of each component's surface. These sensors accurately depict temperature fluctuations on the structure's surface. Influenced by sunlight and environmental factors, the temperature change trend observed by these sensors closely mirrors that of the ambient temperature but lags behind it. As structures at different locations are exposed to varying degrees of sunlight, the temperature changes recorded by sensors exhibit slight variations throughout the day. Given the excellent thermal conductivity of steel and its swift heat transfer capabilities, the temperature monitoring data from the steel structure canopy indicates minimal temperature differences between adjacent measuring points and a consistent change trend, as illustrated

in Figure 3.

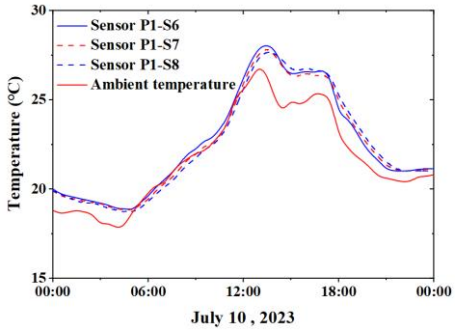

Figure 3: Sensor temperature and ambient temperature

The strain of the awning structure is influenced by various factors, with temperature change being the most critical. As depicted in Figure 4, sensors P1-S6, P1-S7, and P1-S8 at different positions exhibit different responses to temperature variations, resulting in changes in the measured strain. It was observed that the temperature and strain of sensors P1-S6 and P1-S7 are approximately positively correlated, with consistent trends, while the strain and temperature of P1-S8 are approximately negatively correlated. According to the mechanism of temperature-strain change, the effect of temperature on structural strain should be linear [15]. Therefore, we attempt to utilize a linear regression method to fit linear equations of sensor temperature and strain, as illustrated in Figure 5.

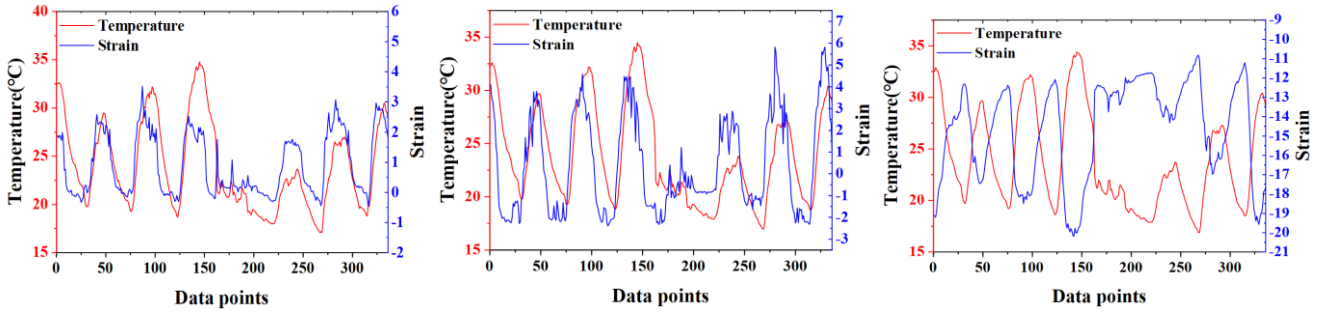

Figure 4: Changes in temperature and strain

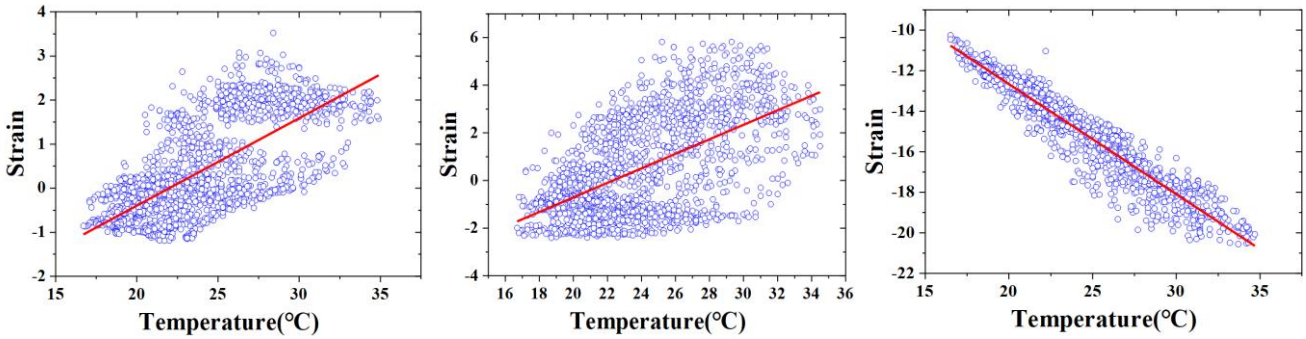

Figure 5: Linear regression analysis of sensor temperature and strain

Through analysis, we have obtained the regression equations for sensor temperature and strain. To assess the fitting effect of the regression model, we employ the goodness of fit R^2. R^2 is a dimensionless value between 0 and 1. The closer the value is to 1, the better the fitting effect of the model and the more reliable the output result. The calculation formula of $R^2$is as shown in formula (1):

$$R^2 = 1 - \frac{\sum_{i=1}^{n}(y_i - \hat{y}_i)^2}{\sum_{i=1}^{n}(y_i - \bar{y}_i)^2} \quad (1)$$

Among them, n is the number of data points,y_i represents the actual measured value of a certain sensor,$\bar{y}_i$ represents the average value of the actual measured values of a certain sensor, and $\hat{y}_i$ represents the regression value of a certain sensor.

The regression line equation for P1-S6 is y=0.2x-4.36, with R^2=0.51. Some points fall on both sides of the fitting line, indicating a poor fitting effect. The regression line equation for P1-S7 is y=0.31x-6.82, with R^2= 0.36. It can be observed that most of the measuring points do not satisfy the equation of the one-variable linear fitting straight line, indicating the worst fitting effect. The regression line for P1-S8 is y=-0.54x-1.81, with R^2=0.93. Most measuring points fall near the fitting straight line, demonstrating an obvious negative correlation between temperature and strain. It can be inferred that for the temperature-strain relationship of the steel structure canopy structure, some measuring points can be better expressed through linear regression. However, there are still a considerable number of measurement points that cannot be represented by a simple linear regression equation.

The strain at a specific location within the structure is influenced not only by the temperature fluctuations in that area but also by the deformation of the surrounding structure. Moreover, the deformation of the surrounding structure is impacted by the temperature at that particular location. Therefore, it is prudent to utilize temperature data collected from multiple sensors to construct a multiple linear regression analysis model. The principle of multiple linear regression is outlined as follows:

Assuming a certain sensor M has monitoring data $\{x_{y1}, x_{y2}, x_{y3}, \ldots, x_{yn}\}$ collected by n sensors during time period t. Additionally, there are k related sensors, and the monitoring values of these k sensors during time period t are represented as:

$\{x_{11}, x_{12}, x_{13}, \ldots, x_{1n}\} \ldots \{x_{k1}, x_{k2}, x_{k3}, \ldots, x_{kn}\}$, Subsequently, the multiple linear regression prediction result can be expressed as:

$$x_{yi} = b_0 + b_1 x_{1i} + b_2 x_{2i} + \ldots + b_k x_{ki} + \varepsilon \quad i = (1,2,3,\cdots,n) \tag{2}$$

In formula (2), x_{yi} is the monitoring data of sensor M, $x_{1i}, x_{2i}, \ldots, x_{ki}$ represent the monitoring data of related sensors,b signifies the partial correlation coefficient, and ε is a random variable. Use the least squares method to obtain the values of $b_0, b_1, \ldots, b_k$ to minimize the sum of square errors between all measured values x_{yi} and regression values, In other words, $Q = [x_{yi} - (b_0 + b_1 x_{1i} + b_2 x_{2i} + \ldots + b_k x_{ki})]^2$ has a minimum value, then the partial regression coefficient can be expressed as:

$$(b_0, b_1, \ldots, b_k)^T = (X^T X)^{-1}(X^T Y) \tag{3}$$

In formula (3)$X = [1, x_{1i}, x_{2i}, \ldots, x_{ki}], Y = x_y$

The prediction accuracy of the multiple linear regression model is evaluated by the goodness of fit R^2. All temperature sensors of the first truss are used to conduct multiple linear regression analyses on P1-S6, P1-S7, and P1-S8. The results are presented as Figure 6:

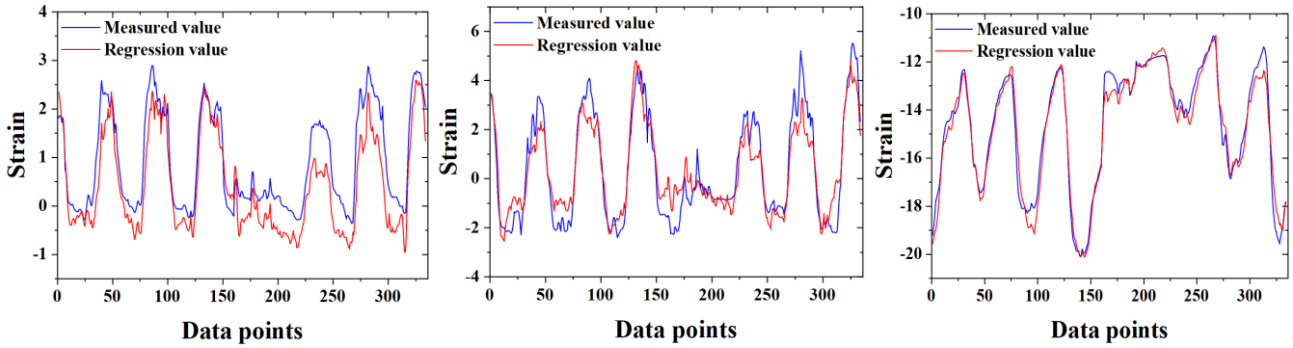

Figure 6: Multiple linear regression results

Multiple linear regression significantly improves the fitting accuracy for temperatures and strains such as P1-S6 and P1-S7 that cannot be analyzed using simple linear regression equations, and the goodness of fit R^2 reaches 0.74 and 0.82 respectively. Although the correlation between temperature and strain of P1-S8 can already be expressed using a linear regression equation, multiple linear regression still improves the fitting accuracy of P1-S8, with R^2 reaching 0.97. To assess the generalization ability of the multiple linear regression model, the equations of P1-S7 and P1-S8 with better fitting effects are utilized to predict 100 data other than the fitted data. The results indicate a significant reduction in prediction accuracy, with R^2 decreasing to 0.67 and 0.95 respectively. The prediction results are shown in Figure 7.

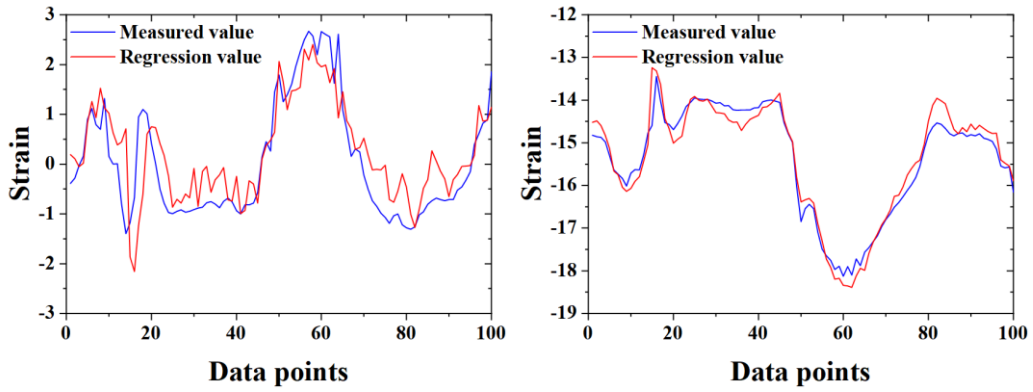

Figure 7: Prediction results

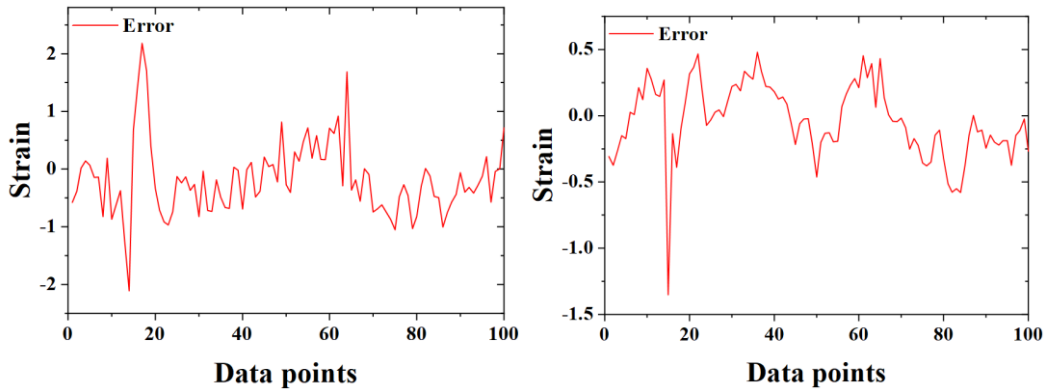

Figure 8: prediction error of P1-S7

Comparing the predicted values and measured values of P1-S7, and drawing the error image as shown in Figure 8, it's observed that the maximum error reaches 2.18 and the absolute average error is 0.5. Although the multiple linear regression model can improve the accuracy of predicting strain based on sensor temperature compared to a single linear regression model, its generalization ability is weak, resulting in low prediction accuracy for unknown data. To address this issue, existing literature suggests that neural networks, with their unique network structure, possess strong mapping capabilities for nonlinear models and robust generalization abilities [7,9,13]. Therefore, this paper aims to construct an LSTM neural network model for Fuyu Station based on the available data.

2.3 Data Preprocessing and Sample Set Data Selection

This paper selects actual measured data from January 2023 to October 2023. These data were collected every half hour in high-speed rail canopies in cold areas, covering the transition from winter to summer. Consequently, they are influenced by both low and high temperature environments, making them representative of temperature and strain changes at Buyeo Station under various environmental conditions. Additionally, the collected data underwent classification, cleaning, and preprocessing operations. For instance, the improved 3σ principle was applied to perform jump filtering of data, and the multiple regression model was utilized to address missing and abnormal data, as shown in Figure 9.

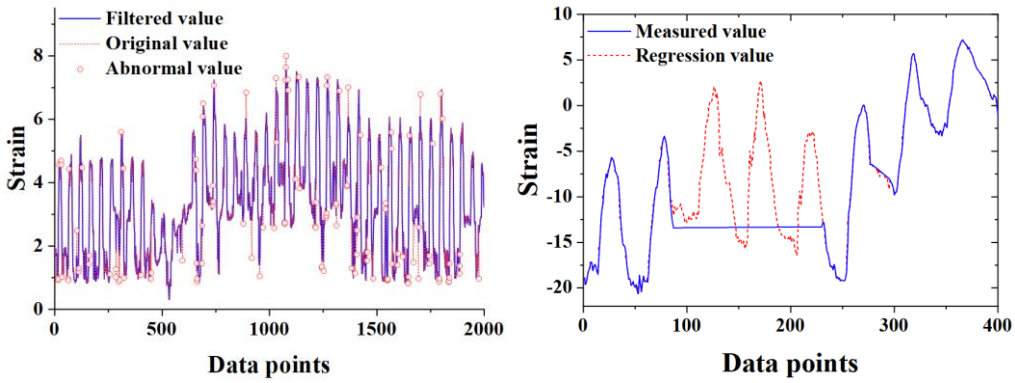

Figure 9: Data preprocessing

3. Construction of Neural Network Model

3.1 LSTM Network Model

Strain changes in a structure are influenced not only by the current temperature but also by temperature variations over time. Therefore, the regression method described earlier is not well-suited to the structural strain characteristics of Buyeo Station. Recurrent Neural Networks (RNNs) are designed to handle such sequential data, performing tasks repeatedly over sequences and forming loops over time. As illustrated in Figure 10, the output at any time step is influenced not only by the current input but also by the inputs from the previous t−1 time steps. This information is stored in the hidden layer h, which facilitates the self-renewal of the cell [11]. However, RNNs face challenges such as gradient disappearance and gradient explosion during backpropagation due to their network characteristics and iterative nature. To address the long-term dependency problem inherent in RNNs, the Long Short-Term Memory (LSTM) network model was developed based on the basic RNN structure. LSTM utilizes a unique memory cell to store and transmit information over long-term dependencies. The structure of the LSTM network is shown in Figure 11.

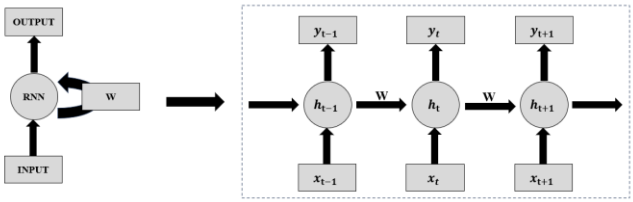

Figure 10: RNN network

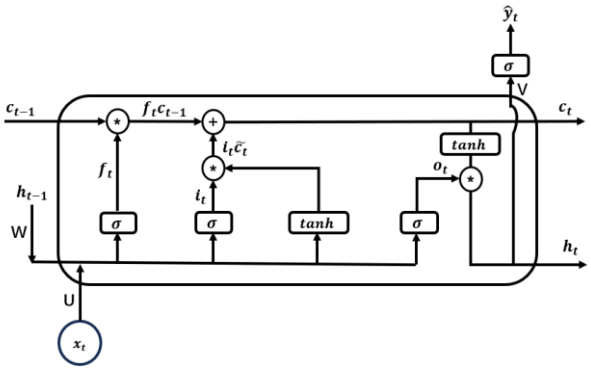

Figure 11: LSTM network

The LSTM cell inherits the characteristics of RNN. The input at the current moment t includes not only the information x_t at the current moment, but also the information h_{t-1} of the hidden layer at the previous moment and the long-term memory C_{t-1} flowing in the cell. The flow of information within the LSTM cell is controlled through a unique structural "gate". Through a series of operations on these gates, the input information is integrated to obtain the output information of the LSTM.

The initial gate is termed the "forget gate". Its primary function is to determine which information the cell ought to discard, consequently influencing the value of the long-term memory C_{t-1}.The operational mechanism of the forget gate can be succinctly captured by the formula as follow:

$$f_t=\sigma(U_f h_{t-1}+ W_f x_t+ b_f) \quad (4)$$

where U_f and $W_f$are the weight matrices in the forget gate;$b_f$is

the bias vector in the forget gate; σ(z) is a logistic sigmoid function used to map values to the [0,1] interval. The σ(z) function is defined by the formula as follow:

$$\sigma(z) = \frac{1}{1+e^{-z}} \quad (5)$$

The second gate is termed the "input gate". Its primary function is to assimilate incoming information into the cell. The operational mechanism of the input gate can be succinctly expressed through the following formula:

$$i_t=\sigma(U_i h_{t-1}+ W_i x_t+ b_i) \quad (6)$$

$$\widetilde{C_t}=\tanh(U_c h_{t-1}+ W_c x_t+ b_c) \quad (7)$$

where U_i,W_i, U_c and W_c are the weight matrices in the input gate; b_i and b_c are the bias vectors in the input gate; tanh(z) is the hyperbolic tangent function used to map values to the [-1,1] interval. The tanh(z) function is defined as follows:

$$\tanh(z) = \frac{e^z-e^{-z}}{e^z+e^{-z}} \quad (8)$$

The third gate, known as the output gate, serves to regulate the information output from the cell. The operational mechanism of the output gate can be represented by the following formula:

$$o_t=\sigma(U_o h_{t-1}+ W_o x_t+ b_o) \quad (9)$$

where U_o and $W_o$are the weight matrices in the output gate, and b_o is the bias vector in the output gate.

The flow and storage of information in LSTM cells can be regulated by the values of the gate parameters. Specifically, the parameter f_t in the forget gate can adjust the long−term memory state of the cell by controlling the retention of the memory cell C_{t-1}.Their product represents the retained long-term information. Similarly, the product of the parameters i_t and $\widetilde{C_t}$in the input gate controls the retention of the current input information. The memory cell C_t can thus be updated in this manner. The update process can be expressed by the following formula:

$$C_t= f_t \cdot c_{t-1}+ i_t \cdot \widetilde{C_t} \quad (10)$$

The result o_t of the output gate and the updated memory cell C_t jointly determine the output value h_t at the current moment. This process is expressed by the following formula:

$$h_t= o_t \cdot \tanh(c_t) \quad (11)$$

3.2 The Establishment Process of LSTM Model

This article presents the development of an LSTM neural network model using Pytorch. Considering the thermal conductivity characteristics of the steel structure canopy, the input data comprises ambient temperature readings collected by weather monitoring stations, rather than the temperature data from each sensor. This approach reduces the volume of input data and minimizes data redundancy in practical applications. For the output data, sensors that are in good condition and effectively represent the canopy's service status were selected. These include P1-S6, P1-S7, P1-S8, P2-S6, P2-S7, and P2-S8. Consequently, a multi-output LSTM neural network model based on ambient temperature and sensor strain was constructed.

Firstly, data preprocessing is necessary to acquire a well-conditioned dataset. Secondly, to enhance the network's learning capability and accelerate convergence, normalization of both input and output data is required. The normalization formula for input and output data is as follows:

$$X_t = \frac{X_t-X_{min}}{X_{max}-X_{min}} \quad (12)$$

$$Y_t = \frac{Y_t-Y_{min}}{Y_{max}-Y_{min}} \quad (13)$$

Among them,X_t and Y_t represent the real values at time t; X_{max} and Y_{max}denote the maximum values of the input and output data, respectively; X_{min} and Y_{min} represent the minimum values of the input and output data, respectively.

The training process of the neural network is conducted using the iterative optimization method of multiple epochs. In each epoch, the loss calculated from the regression value and the true value serves as the basis for gradient descent. The parameters in the network are continuously optimized during the gradient descent process, which constitutes the backpropagation process of the neural network. The calculation of loss and the process of backpropagation are closely related to the choice of loss function. The LSTM network model constructed in this article utilizes mean square error (MSE) as the loss function to participate in the backpropagation of gradients. The calculation formula of MSE is as follows:

$$MSE = \frac{1}{n}\sum_{n=1}^{N}(y_i - \hat{y_i})^2 \quad (14)$$

where N is the number of samples,$y_i$is the measured value, and $\hat{y_i}$ is the regression value.

This article selects actual measured data collected every half hour from high-speed rail canopies in cold areas from 0:00 on January 1, 2023, to 15:30 on October 19, 2023. The dataset is divided as follows: the first 11,000 data points are designated as the training set, while data points 11,001 to 12,000 are allocated to the validation set, used to assess the model's performance on unseen data during the training process. The last 2,000 data points constitute the test set, utilized to evaluate the predictive performance of the model.

The hyperparameters of neural networks play a crucial role in determining model performance, necessitating a balance between training time and accuracy. In this article, the selected hyperparameters are as follows: the model adopts a two-layer LSTM hidden layer structure, with each layer containing 128 neurons. To prevent overfitting, a dropout layer is incorporated with a dropout rate of 0.1. The batch size is set to 32, and the Adam optimizer is utilized during backpropagation. Time steps significantly influence model accuracy, with an increase in time steps leading to longer training times. After conducting numerous experiments, this article ultimately establishes the time step as 30, wherein a temperature sequence comprising 30 time steps is input, and each sensor outputs the corresponding temperature-induced strain.

The number of iterations is set to 200. Upon reaching 200 iterations, the training concludes, and the model exhibiting the best performance on the validation set is saved to enhance the model's generalization ability.

3.3 Prediction Results based on LSTM Model

The prediction accuracy of the model is evaluated using the root mean square error (RMSE) and the coefficient of determination (R^2). The prediction results are presented in the following table:

Table 1: The prediction results

Sensor id	P1-S6	P1-S7	P1-S8	P2-S6	P2-S7	P2-S8
RMSE	0.3945	0.6450	0.5144	0.3939	0.6958	0.6044
R^2	0.8907	0.8995	0.9699	0.9349	0.8477	0.8944

For instance, considering P1-S6 and P1-S7, the prediction outcomes for these sensors are illustrated in the figure below:

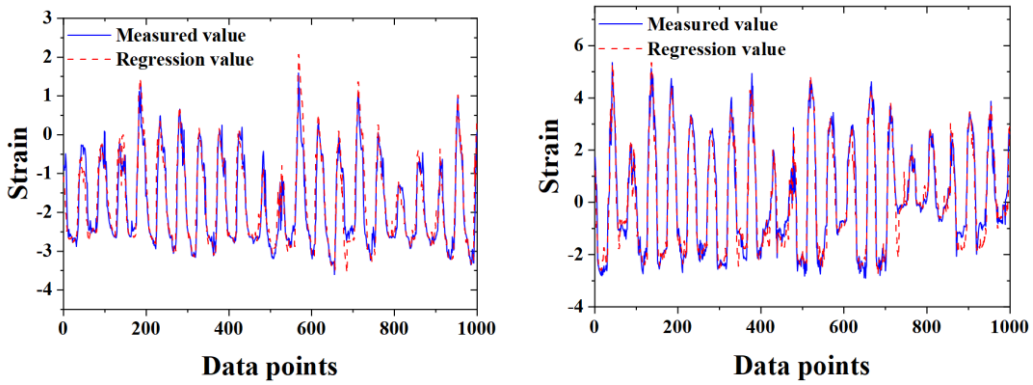

P1-S6 P1-S7

Figure 12: Prediction results of P1-S6 and P1-S7

The capabilities of LSTM in capturing the intricate mapping relationship between ambient temperature and strain, as demonstrated in the examples presented in this article, underscore its potential for predicting structural strain changes effectively. Leveraging this, it becomes feasible to forecast strain at multiple measurement points within the structure. By comparing real values with the predicted values generated by the network, real-time warnings can be issued.

4. Conclusion

1) The stress-strain relationship of the structure is not a simple linear relationship and cannot be expressed simply by linear equation.

2) Deep learning models excel at capturing intricate temperature-strain relationships, facilitating the prediction of strain variations based on temperature fluctuations.

3) LSTM neural network can predict the strain change of structure with remarkable effect, which is of great significance to the prediction and early warning of practical engineering

References

[1] Lightweight Network Communication of Railway Health Monitoring System Based on BIM Model[J].
[2] Behavior Analysis and Early Warning of Girder Deflections of a Steel-Truss Arch Railway Bridge under the Effects of Temperature and Trains Case Study[J].
[3] Fiber optic health monitoring and temperature behavior of bridge in cold region[J].
[4] In-Service Condition Assessment of a Long-Span Suspension Bridge Using Temperature-Induced Strain Data[J]. Journal of Bridge Engineering, 2016, 22(3).
[5] Recent Progress of Fiber-Optic Sensors for the Structural Health Monitoring of Civil Infrastructure[J].
[6] Hanwen Ju, Wenqiang Zhai, Yang Deng, et al. Temperature time-lag effect elimination method of structural deformation monitoring data for cable-stayed bridges[J]. Case Studies in Thermal Engineering, 2023, 42: 102696.
[7] Smriti Sharma, Subhamoy Sen. Real-time structural damage assessment using LSTM networks: regression and classification approaches[J]. Neural Computing and Applications, 2022, 35: 557-572.
[8] Md Abdullah Al Mehedi, Achira Amur, Jessica Metcalf, et al. Predicting the performance of green stormwater infrastructure using multivariate long short-term memory (LSTM) neural network[J]. Journal of Hydrology, 2023, 625: 130076.
[9] Jian Zhang, Jianliang Zhang, Zhishen Wu. Long-Short Term Memory Network-Based Monitoring Data Anomaly Detection of a Long-Span Suspension Bridge [J]. Sensors: 1-17.
[10] Guifeng Zhao, Hui Qian, Kaifeng Xing, et al. Long Short-Term Memory Network for Predicting Wind-Induced Vibration Response of Lightning Rod Structures[J]: 1-22.
[11] Deep learning in neural networks: An overview[J].
[12] Long Short-Term Memory[J].
[13] Mechanics-Guided optimization of an LSTM network for Real-Timemodeling of Temperature-Induced deflection of a Cable-Stayed bridge[J].
[14] A multi-sensor mapping Bi-LSTM model of bridge monitoring data based on spatial-temporal attention mechanism[J].
[15] General formulas for estimating temperature-induced mid-span vertical displacement of cable-stayed bridges[J].